EUROPEAN ORGANIZATION FOR NUCLEAR RESEARCH

CERN/SPSC 84-13
SPSC/P196
29 February 1984

P R O P O S A L

THE PRODUCTION OF STRANGE BARYONS AND ANTIBARYONS WITH RELATIVISTIC LIGHT ION COLLISIONS AT THE CERN SPS

C.R. Gruhn[1(*)], M. Heiden[1], G. Løvhøiden[2], G.C. Morrison[3], H.G. Pugh[1], W.D.M. Rae[4], T.J.M. Symons[1] and T.F. Thorsteinsen[2]

1 Lawrence Berkeley Laboratory, Berkeley, CA, USA
2 University of Bergen, Bergen, Norway
3 University of Birmingham, Birmingham, UK
4 University of Oxford, Oxford, UK
(*) Spokesman

ABSTRACT

We propose to measure the inclusive production cross sections of strange baryons and antibaryons with light ion collisions with nuclear targets (A = 9-238) over the energy range of 13 GeVA to 200 GeVA at the CERN SPS. A high-field superconducting magnet would be used to disperse the high multiplicity of mesons from the region of our measurement. A micro TPC would be used to recognize primary decay kinks and secondary decay V^o's.

1. INTRODUCTION

The construction by Lawrence Berkeley Laboratory (LBL) and Gesellschaft für Schwerionenforschung Darmstadt (GSI) of an injector for the CERN SPS opens extraordinary opportunities for the study of high energy nucleus-nucleus collisions. Beam energies up to 225 GeVA will be available.

LBL and GSI are presently approved for an experiment (PS190) using a streamer chamber and the plastic ball. The terms of the LBL-GSI-CERN Agreement concerning the ion source include availability of the beam to all comers. Already letters of intent and proposals have been submitted by others. We have devised an experiment to measure the production of strange baryons and antibaryons [P, Λ, Σ, Ξ, Ω ($|S| = 0, 1, 2, 3$)]. In addition, we will measure the production of K^0_s. In particular, the production of $|S| = 3$ (Ω(sss)) is expected to have the least bias to correlations in light quark (u,d) production and therefore may be the most sensitive signature (with enhanced production) of the quark-gluon plasma.

This proposal states briefly the physics motivation and goals in sect. 2, beams and beam line in sect. 3, targets in sect. 4, experimental design and apparatus in sect. 5, triggers in sect. 6, acceptances in sects 7 and 8, rates and sensitivity in sect. 9, a run plan and request in sect. 10, Monte-Carlo event simulation in sect. 11, support in sect. 12 and conclusions in sect. 13.

2. PHYSICS MOTIVATION AND GOALS

It is proposed to measure the production of strange quarks in nucleus-nucleus collisions as a signal of the formation of a quark-gluon plasma (QGP). A number of workshops, reviews, lectures and papers concerning the subject of "quark matter" or "quark-gluon plasma" have been published recently [1-4] and serve to motivate the physics proposed. From this compendium of work some rather general conclusions can be reached:

(a) The critical energy density for formation of the QGP is expected to lie somewhere between 1/2 GeV/fm^3 and 2 GeV/fm^3.

(b) At energies below ~ 10-50 GeVA a heavy target nucleus (uranium) is expected to stop the projectile producing energy densities up to 1-1.5 GeV/fm^3 [4].

At energies above ~ 10-50 GeVA the nuclei assume a partial transparency. However, some of the produced particles are expected to thermalize in the target and projectile fragments leading to energy densities of ~ 1 GeV/fm^3. The energy density in the central region is expected to be ~ 2 GeV/fm^3 and the quark-antiquark populations are about equal.

(c) The most promising signals of a QGP are those which are least affected by final state interactions.

(i) Weakly interacting produced particles - single photon and dilepton production.

(ii) Quantum numbers which remain unchanged by strong interactions - strange quark production [2,3].

We plan to focus on this last signal, the production of strange quarks and antiquarks. The recent lectures of Müller [3] summarize very well the various aspects of strangeness as a signature for the QGP. It is pointed out that from existing pp data the relative abundances of strange to non-strange quarks and antiquarks for the "hadronic phase" at 14.5 GeV are

$$N_s/N_q = 0.007, \quad N_{\bar{s}}/N_{\bar{q}} = 0.017 .$$

For the "QGP phase" he calculates

$$N_s/N_q = 0.035, \quad N_{\bar{s}}/N_{\bar{q}} = 0.5 .$$

The result is a factor of 5 and 30 enhancement in the respective relative densities.

Müller [3], as others [2], suggests the particle production ratio $\bar{\Lambda}/\bar{p}$ or even $\bar{\Omega}/\bar{\Lambda}$ as a sensitive indicator for this enhancement in strangeness production.

Our experiment is designed to be sensitive to strangeness production in general with special emphasis on the inclusive production cross sections of strange baryons and antibaryons [P,Λ,Σ,Ξ,Ω ($|S|$ = 0,1,2,3)] in the central and projectile fragmentation regions. In addition we will be sensitive to K^{o}_{s} production. The study of strange baryons and antibaryons and the measurement of the production ratios gives evidence on the relative densities of strange and non-strange quark and antiquarks in the reaction volume. An example of such ratios is P:Σ:Ξ:Ω which should be a simple sequence corresponding to the composition of those particles: (qqq):(qqs):(qss):(sss). The antiparticle production ratios are expected to be different because while one may expect $\bar{s}$ production to equal s production the number of q(u,d) and $\bar{q}$ quarks in the final state will be different because of the large number of q quarks already present before the collision. Many such ratios have been measured for pp and p-nucleus collisions and several phenomenological models have been devised to explain them. Our experiment would add information for a new range of parameters which will be valuable irrespective of whether a new state of matter is formed.

We propose to study strangeness production spanning an energy range where "nuclear stopping" and baryon density is a maximum and strange antibaryon production is at threshold up to the highest SPS energies (7-225 GeVA). See table 1 for the threshold energies of strange baryon-antibaryon production.

3. BEAMS AND BEAM LINE

It is our desire (within the constraints of this experiment) to stay compatible with the presently approved LBL-GSI experiment (PS190) using a streamer chamber in the SPS West Experimental Area beam H3 and plastic ball in the X5 beam. These beams are designed as test beams [5] for the LEP Detectors (L3 beam X3, OPAL beam X5, DELPHI beam X7A and ALEPH beam X7B). The H3 beam is split three ways between X3, X5, and X7 with a double magnetic split.

In its present form the beam will be shared between the streamer chamber (H3) and the plastic ball (X5) (PS190); the top and bottom of the three way split. The remaining middle portion of the beam is sent to X7,

the ALEPH test beam. We propose to use this beam, X7, with the permission of ALEPH. We hope to be able to run simultaneous to the experiments in H3 and X5B. We request running at 13, 40, 75 GeVA, 200 GeVA with priority in the same order (13 GeVA highest). However, if PS190 requests running at < 13 GeVA (7GeVA) we would use this beam to study subthreshold strange baryon antibaryon production.

The beam line X7A in its present form has a maximum momentum capability of 75 GeV/c per nucleon. We propose use of all light ion beams (^{4}He to ^{16}O, and heavier ions). We hope that our experiment be phased between the foreseen low energy running (first) and hopefully the higher energy running which would follow. We request to move our experiment to a more appropriate beam line for the highest energy run (≦ 200 GeVA) (arrangements to be made after the lower energy running).

From the experimental viewpoint starting with lowest energy is easiest since the multiplicities are least and the forward cone opening angle is largest. From the physics point of view it is not completely clear what the optimum energy will be. Thus, the low energy running would allow us to gain experience in the accommodation problems and thus adapt the detector and detection algorithms for the highest multiplicities at the highest energies.

4. TARGETS

It is our goal to study the strange baryon antibaryon production over as large a range in target mass (A) as possible [^{9}Be, ^{27}Al, Ni, ^{120}Sn, ^{208}Pb, U]. The target must be chosen thin such that the high multiplicities of produced pions, projectile and target fragments have a low probability of producing a secondary reaction in the target. We chose a target such that we have a ≦ 10% chance that one of these primaries interact in the target. This thickness represents a compromise between backgrounds produced elsewhere and interaction rate.

In table 2 we list some of the relevant material properties of the targets. In table 3 we give the interaction cross sections assuming an ^{16}O beam and probabilities for targets having a 0.1% collision length

thickness. In table 4 we give the interaction probabilities for the target thicknesses yielding ≤ 10% chance for a secondary interaction in the target assuming a 13 GeVA ^{16}O beam and for near zero impact parameters. At higher energies the targets would be chosen thinner in inverse proportion to the multiplicity.

5. EXPERIMENTAL DESIGN AND APPARATUS

The detection of strange baryons and antibaryons is complicated by the fact that they have relatively short decay lengths (2.4 cm ≤ $c\tau$ ≤ 7.9 cm). This forces a compact experimental design in order to have reasonable efficiencies at the lower projectile energies (13 GeVA) and even for the highest projectile energies (~ 200 GeVA). We have the additional complication that the events most desirable for study are those with a maximum number of nucleons participating which will have very high multiplicities in the laboratory forward cone. Charged particle multiplicities of several hundreds are expected at the highest energies. See table 5 as a rough example of multiplicities and rapidity densities expected. For pp collisions one has the mean multiplicity, η_o and the central rapidity density ρ_o

$$\eta_o = 0.88 + 0.44\ \ell ns + 0.11\ (\ell ns)^2 \qquad (1)$$

and

$$\rho_o = \frac{1}{3}\ (-0.07 + 0.74\ \ell ns)\ . \qquad (2)$$

In nucleus-nucleus collisions a simple minded approach scales the multiplicity and rapidity density with the number of nucleon-nucleon collisions. In sect. 11 we discuss this approach. For a light projectiles (A = 16, 40) on a heavy target the number of nucleon-nucleon collisions per nucleus-nucleus collision is ~ 16 or 40.

Although ^{16}O beams are anticipated for 1986 in the SPS [6], heavier ion beams are expected to follow in the subsequent years. Therefore, we propose an experimental design which will accommodate the very high multiplicities expected for the interactions of these heavier ion beams. Not all of the nucleons will participate and therefore we must anticipate a large number of target and projectile fragments which also appear in the laboratory forward cone.

Since the major portion of the high multiplicity is associated with mesons which are light compared to the baryons we will use a magnetic filter to sweep away the lower momenta from the forward cone. In order to achieve a compact design we will use a high-field superconducting magnet to disperse the high multiplicity of mesons, target fragments, and projectile fragments from the region of our measurement.

A filter magnet design having as wide a gap (material free) possible and low field 3.5 T over 30 cm diameter is proposed for the lowest energies $\leq$ 13 GeVA and narrower gap but with high field 7 T for the highest energies $\geq$ 40 GeVA. This variable gap superconducting magnet is placed with the target at its edge as shown in fig. 1.

In the relatively particle free region beyond the filter magnet we will place a micro TPC to detect the $B\bar{B}$ production. The μTPC follows the design of the ALEPH central detector TPC in terms of electronics and sense pad design thus allowing both this effort and ALEPH to benefit from a common set of detector experience. The μTPC is placed adjacent to the beam and dispersed nuclear projectile fragments. It sees momenta greater than ~ 2 GeV/c in the forward cone. Its geometry is such as to allow for both recognition of a primary decay kink and a secondary decay V^{o}. Beyond the μTPC we place three planes of drift chambers to provide enhanced momentum measurement resolution. This is followed by a Cherenkov threshold detector hodoscope used in the trigger.

On each side of the filter magnet we place a multiplicity detector which will sample the number of particles having parallel momenta less than 1 GeV/c. Some distance in front of the target is placed a Cherenkov beam tag detector. The target (charged) fragments are swept to one side of the beam and are detected in a target fragment detector. The projectile fragments are dispersed about the beam (q/m ~ 1/2) and their energy is measured in a calorimeter down stream.

The total path along the beam required is less than 5 m in X7B.

6. TRIGGERS

There are three triggers which we plan to use; a minimum bias, an impact parameter or central collision, and an antibaryon or strange baryon trigger.

6.1 Minimum bias trigger

The minimum bias trigger will consist of a valid beam tag in coincidence with any charged particle leaving the μTPC detected by a scintillator having a signal greater than ~ 1/2 Min.I. The expected rate of such triggers is about the beam interaction rate.

6.2 Central collision trigger

The central collision trigger will consist of a valid beam tag in coincidence a low energy detected in the nuclear projectile fragment energy calorimeter. If needed the multiplicity tag can be added to this trigger. Geometric considerations show that head on collisions [7] ($b \leq 1$ fm) comprise $(1/2R)^2$ of the nucleus-nucleus collisions ($\geq 0.5\%$). This trigger rate is ~ 0.05 of the interaction rate.

6.3 Antibaryon or strange baryon trigger

This trigger will consist of a valid beam tag in coincidence with the detection of a proton or antiproton beyond the μTPC with a geometric cut which excludes protons from the target (except for high p_T protons). The $p(\bar{p})$ will be detected in a scintillator-Cherenkov detector hodoscope. This geometric cut will be placed such that at least 1/2 of the triggers will come from antiprotons produced in the target. The trigger will be designed to accept a large fraction of strange baryon and antibaryon production. The trigger rate is expected to be about that of the anti-proton production rate.

7. ACCEPTANCES

The design goal is to have the highest possible acceptance relative to background particles over a rapidity range of $y^* = 0$ to $y = y_{beam}$ and the angular range $0^\circ \leq \theta \leq 90^\circ$. The acceptance is further complicated by the fact that some of the particles decay to particles (neutral) not

detected and some particles have both a primary and a secondary decay, both of which which we must recognize in the detector system.

For this reason we divide the acceptance into a product of factors $P_p \times P_s \times DF \times K$, where

- P_p is the probability that the primary decay is observed,
- P_s is the probability that the secondary decay is observed,
- DF is the useable decay fraction product for both primary and secondary decays,
- K is the kinematic acceptance (rapidity and p_T interval) accepted.

In table 6 we give the relevant decay fractions (DF) for the strange baryons. Note, we do not detect neutrons or π^o.

In tables 7(a-d) we give the probability that the primary particle survives decay up to a given distance for central rapidity ($y^* = 0$) at the beam momenta of 13, 40, 70, 200 GeV/c/nucleon.

In table 8(a-d) we give the efficiency of the detector to detect the decays A_D at $y^* = 0$ and for the beam momenta of 13, 40, 70, 200 GeV/c/nucleon. These results are shown graphically in fig. 2 as a function of the laboratory momenta of the particles. It is clear that using the acceptance calculated at $y^* = 0$ is an underestimate for $y^* > 0$.

We next consider the kinematic acceptance K.

$\bar{p}$ we accept about 1/2 of the forward hemisphere or K = 0.25.

$\Lambda\bar{\Lambda}$ we accept $p_T/p_{||} \geq 0.066$ over 1/2 the sphere at $y^* = 0$

p_{beam} (GeV/c)	K
13	0.24
40	0.13
70	0.085
200	0.024

Σ^+ we accept $p_T \geq P_{FM}$ over 1/2 of the forward hemisphere

$p_T = 0.32$ for $\leq$ 13 GeV/c, K = 0.07

$p_T = 0.64$ for $\leq$ 40 GeV/c, K = 0.02

Σ^- we accept 1/2 of the forward hemisphere K = 0.25,

Ξ^- we accept ~ 1/2 of the forward hemisphere K = 0.25,

Ω^- we accept ~ 1/2 of the forward hemisphere K = 0.25,

K^o_s our kinematic acceptance is about the same as for $\Lambda\bar{\Lambda}$.

8. BACKGROUND ACCEPTANCES

The main background is associated with those particles from the target which are not swept free of the μTPC by the filter magnet. The majority of positive particles passing the filter are protons where we accept 1/2 of the forward hemisphere with $p_T \geq 0.32$ at $\leq$ 13 GeV/c/nucleon and $p_T \geq 0.64$ at $p_{beam} \geq 40$ GeV/c/nucleon.

$p_{beam} \leq 13$, K = 0.07,
$p_{beam} \geq 40$, K = 0.02.

The majority of negative particles passing the filter are π^- having $y_{lab} \geq 2.3$ and $p_T \leq 0.32$ for $p_{beam} \leq 13$ GeV/c/nucleon and $y_{lab} \geq 3.0$ for $p_T < 0.64$ for 1/2 of the forward hemisphere.

p_{beam} (GeV/c)	K
13	0.04,
40	0.02,
70	0.026,
200	0.04.

In figs 3 and 4 we show the results of the background detected at 13 GeV/c/nucleon superimposing 16 nucleon-nucleon collisions. See sect. 11 for the discussion.

What is clear is that with almost every interaction we will have some particles in the μTPC.

9. RATES AND SENSITIVITY

In order to estimate the data rates we make the following assumptions: beam intensity is 10^6 ions/pulse. Acceptance A is calculated at $y^* = 0$. Fig. 2 shows this to be underestimated for higher rapidities. Multiplicity is for a single pp collision (table 9). Target interaction

probability T is such that ≦ 10% of primary particles produced have a secondary interaction in the target.

The rate is then calculated as

$$R(B,p_b) = 10^6 \cdot A(B,p_b) \cdot \langle B,p_b \rangle_{pp} \cdot T(B,p_b) \cdot$$

In table 10 we give the detected particle rate $R(B,p_b)$, for given values of the acceptance A, the multiplicity in a single pp collision, $\langle B,p_b \rangle_{pp}$ and the target interaction probability T for an ^{16}O beam.

This rate must be scaled upward by a factor which gives the mean number of NN collisions per target interaction (~ 8-16 for light-heavy targets). Assuming 10^4 beam pulses per day we may expect the following approximate event numbers for $^{16}O + U \rightarrow B + X$ at 13 GeVA $\bar{p}(10^5)$ $\Lambda(1.2 \times 10^5)$ $\bar{\Lambda}(69)$ $\Sigma^+(38)$ $\Sigma^-(4.2 \times 10^3)$ $\Xi^-(1.5)$ and at 40 GeVA $\bar{p}(4.2 \times 10^5)$ $\Lambda(4.3 \times 10^5)$ $\bar{\Lambda}(0.9 \times 10^4)$ $\Sigma^+(10^3)$ $\Sigma^-(8.6 \times 10^4)$ $\Xi^-(540)$ $\Omega^-(26)$.

In all cases the lighter targets are more efficient. <u>These rates are the rates we would expect if there is no enhancement (no QGP)</u>. It is clear that the rates are such that the enhancement factor of Müllers would be observed even if the QGP is created only for impact parameters of less than 1 fm.

10. <u>RUN PLAN AND REQUEST</u>

We would take approximately 10^5 events for each of the three triggers (minimum bias -1 h, central -2.5 h, B-B -24 h or 1.2 days) for each of 7 targets and 2 energies for a total of 17 days. Our highest priority momentum is 13 GeV/c/nucleon for this first run. Our second choice momentum is 40 GeV/c/nucleon, however, if PS190 runs 7 GeV/c/nucleon we would request to take data concurrently. An acceptable run plan would be for 17 days at ≦ 13 GeV/c/nucleon during the low power period of 1986, and 10 days of 40 GeV/c/nucleon and 7 days of 75 GeV/c/nucleon in a following SPS run period. If less running time is available we would look at less targets. We will require three days of set up time. We also request an equivalent amount of time when beams heavier than ^{16}O are available. After completion of the low energy phase of the experiment we would request

225 GeV/c/nucleon in an appropriate beam line where we would move the experiment.

The experiment depends upon having a calibrated acceptance of the apparatus and triggers. In order to achieve this, we request protons of the same momentum (13 GeV/c) for a period of 5 days just prior to the light ion run. We would request a hydrogen target to be available for 2 of the 5 days.

We would also take p nucleus data for at least 2 of our targets as a part of the calibration.

In addition, test beam time will be required in order to debug the detectors, electronics, trigger etc. We require 42 days of test beam time in X7B (spread over a period of ~ 1 1/2 years prior to the run). Most of the tests and apparatus is thin (< 0.1 L_{rad}) and will be contained in a 5M length along the beam. It is anticipated that considerable cooperation with the ALEPH LEP detector testing will be required.

The data will be analyzed mainly with the computing facilities of the collaborating institutions. One hundred hours of CERN IBM time is requested between now and during the time of the experiment to aid in the development of the μTPC and for check runs.

11. MONTE-CARLO EVENT SIMULATION

We do not attempt to undertake a precise nucleus-nucleus Monte-Carlo event simulation. Rather, we try to simulate the type of production one might expect in the situation where all the projectile nucleons collide in single collisions independently with target nucleons at rest (no Fermi motion assumed). We feel that this represents the situation of a near zero impact parameter, but with an overestimate of the energy flow into the forward hemisphere where this experiment tends to focus. Since we only use the Monte-Carlo simulation at this point to estimate backgrounds (overestimation) we feel this procedure is safe.

In figs 3 and 4 we show an event with only those charged particles which traverse the μTPC. This event was generated by superimposing 16

nucleon-nucleon collisions at 13 GeV/c. The total number of tracks including neutrals for the event was 137. The number of charged tracks passing through any portion of the μTPC was 10 which also included an e^+e^- pair from γ pair production in material before the detector. Other configurations of the filter magnet μTPC geometry are being considered for the higher energies. The very high multiplicities for the events of interest make the backgrounds and trigger considerations difficult and demonstrate the need for the filter magnet in this type of experiment.

12. SUPPORT

A major portion of the support for this experiment is expected to come from LBL including the construction and testing of the detector system. Because of the size of the experiment and resource needs we are considering further collaborations with CERN member states and CERN and would welcome other groups. The detector and electronics development on TPC done with the ALEPH LEP Collaboration is to be conducted in a mutually beneficial manner resulting in cost savings. Some aspects of the detector development will also take advantage of test beams at SLAC. LBL will supply the filter magnet. We are seeking to borrow a large dipole magnet from CERN for the μTPC.

13. CONCLUSIONS

We have proposed to measure the inclusive production cross sections of strange baryons and antibaryons with light ion collisions with nuclear targets (A = 9-238) over the energy range of 13 GeVA to 200 GeVA at the CERN SPS.

We expect to detect per day the following approximate event numbers for $^{16}O + U \rightarrow B + X$ at 40 GeVA [K^o_s(2200) $\bar{p}(4.2 \times 10^5)$ $\Lambda(4.3 \times 10^5)$ $\bar{\Lambda}$(9000) Σ^+(1000) $\Sigma^-(8.6 \times 10^4)$ Ξ^-(540) Ω^-(26)]. <u>These rates are the rates we would expect if there is no enhancement (no quark-gluon plasma)</u>. It is clear that the rates are such that the predicted enhancement factor would be observed even if the quark-gluon plasma is created only for impact parameters of less than 1 fm.

A high-field superconducting magnet would be used to disperse the high multiplicity of mesons from the region of our measurement. A micro TPC would be used to recognize primary decay kinks and secondary decay V^{o}'s.

APPENDIX A

DESCRIPTION OF DETECTORS AND MAGNETS

A1. Beam tag detector

The beam line is designed to pass a given charge to mass ratio Z/A at a fixed $\beta\gamma$. The most probable nuclear interaction in material in the beam path is nuclear projectile fragmentation. All the fragments produced having the same Z/A as the beam will appear as a beam contaminant. This is the reason for an efficient beam tag. T.J.M. Symons (on this proposal) has developed a 6 mm thick Lucite Cherenkov detector which is quite sensitive to the Z of the projectile. At Z = 26 he measures the charge resolution σ_Z = 0.15 units of charge. For ^{16}O ions we would expect $\sigma_Z \simeq 0.3e$ for the same radiator length.

A2. Micro TPC

The idea here is to make a TPC design which is equivalent to a ϕ wedge (~ 0.37 radians) taken from the LEP ALEPH TPC central detector. We will standardize to the ALEPH design on gating grid, shielding grid, sense and field wire plane, and cathode sense pad layout. We will keep the drift distance to 30-50 cm thus minimizing the clear time to ~ 10 μs and reducing the field cage voltage to less than 10 kV. A thin field cage ($\leq$ 0.01 Lrad) is expected to be achieved.

In the summary session of the Third International Conference on Ultra-Relativistic Nucleus-Nucleus Collisions, W. Willis discusses the question of tracking for very high multiplicities. As an example, he shows the simulation of a jet of 50 GeV in the ALEPH detector for LEP. The density of charged particles in these jets is ~ 10^3 per steradian which is similar to that which we would expect in a normal nucleus-nucleus collisions at $\sqrt{s}$ ten times higher than that proposed here. In this example ALEPH predicts a fraction of wrongly assigned points in such a particle density of less than 1%.

In our design we reduce the number of particles to be tracked to a value comparable to the number of tracks expected to be readout by ALEPH (a few tens).

A3. Cherenkov threshold detector hodoscope

The purpose of this detector is two fold. Firstly, it will be used as a part of the trigger for $\bar{p}$ and p or $\bar{p}$ from Λ or $\bar{\Lambda}$ decays. Secondly, we will use it to extend the particle identification capability of the μTPC. A threshold $\beta_T \simeq 0.93$ will be used corresponding to ~ 0.35 GeV/c pions, 1.25 GeV/c kaons and 2.37 GeV/c protons. The design will require a high resolution or maximum number of photoelectrons in order to set a clean cut with a veto on pions at ~ 1.0 GeV/c. This cut will impact our efficiency in the fragmentation region for this trigger. Each Cherenkov module will protect a scintillator which will tell when a particle is passing. The trigger is $S\bar{C}$.

A4. Beam and projectile fragment calorimeter

The purpose of this calorimeter is to measure beam and projectile fragment energy which did not participate in the collisions. It will out of necessity be a high rate device, probably a scintillator-iron sandwich using a wave shifter readout scheme.

A5. Multiplicity and target fragment detectors

These detectors will consist of a sandwich of lucite radiators and scintillators each viewed separately by PM tubes. The net scintillation and Cherenkov light observed is expected to be proportional to the total number of charged particles passing the sandwich.

A6. Superconducting filter magnet

The purpose of this magnet is to deflect from the region of the μTPC low momenta particles (predominantly pions) thus reducing the amount of tracking of background particles.

We are seeking a commercial supplier for this magnet. Presently, American Magnetics Corporation is undertaking the design. Some general features which we hope to incorporate in the design are:

- field length 30 cm,
- variable gap,
- material free gap,
- magnetic field 3.5 - 7.0 T,
- return path for field.

REFERENCES

[1] General references:

M. Jacob and H. Satz (eds), Quark matter formation and heavy ion collisions, World Scientific Publishing Co., Singapore (1982);

R. Bock and R. Stock (eds), Workshop on future relativistic heavy ion experiments GSI-Report 81-6;

The TEVALAC, LBL PUB 5081 (1982).

[2] J. Rafelski, Strangeness production in the quark-gluon plasma, CERN/TH 3745 (1983);

J. Rafelski, Strangeness and phase changes in hot hadronic matter, LBL-16281 and CERN/TH 3685 (1983).

[3] Berndt Müller, The physics of the quark-gluon plasma, UFTP 125/83.

[4] W. Busa, Fragmentation data in hadron-nucleus collisions: implications about nuclear stopping power, proceedings quark matter 1983, Nucl. Phys. A (to be published);

W. Busza and A. Goldhaber, Institute for theoretical physics report, ITP-SB-82-22 (to be published).

[5] D.E. Plane, The west area beams, CERN/SPS 83-22 (EBS) and Technical Report CERN/SPSC 83-36, SPSC/T25 (9 May 1983).

[6] H. Haseroth, Light ions in the PS-complex, CERN/PS/LR 81-27 (23 June 1981);

W.C. Middelkoop, Remarks on the possible use of the SPS for ^{16}O ion beams, CERN/SPS/AC/WCM/Tech. Note 82-1 (22 September 1982).

[7] L. McLerran, The quark-gluon plasma and nucleus-nucleus collisions, Fifth high energy heavy ion study, LBL-12950 (May 1981).

[8] The multiplicities shown here are interpolated from the following references:

M. Bourquin et al., Nucl. Phys. B153 (1979) 13;

M. Bourquin et al., Zeitschr. für Phys. C5 (1980) 275;

V. Blobel et al., Nucl. Phys. B69 (1974) 454;

H. Kichimi et al., Phys. Review 61B (1976) 37;

F.W. Büsser et al., Phys. Rev. D11 (1975) 1733;

K. Jaeger et al., Phys. Rev. D11 (1975) 1756;

K. Jaeger et al., Phys. Review D11 (1975) 2405;

M. Antinucci et al., Lett. al Nuovo Cimento 6 (1973) 121.

TABLE 1

Threshold c.m. energies and beam momenta for the reaction $pp \rightarrow pp B\bar{B}$

$B\bar{B}$	$\sqrt{s}$ GeV	p_{beam} GeV/c
$p\bar{p}$	3.753	6.5
$\Lambda\bar{\Lambda}$	4.108	8.0
$\Sigma\bar{\Sigma}$	4.271	8.8
$\Xi\bar{\Xi}$	4.519	9.9
$\Omega\bar{\Omega}$	5.221	13.6

TABLE 2

Target material properties

Material	L_{coll} (cm)	L_{rad} (cm)	ρ g/cm^3	0.1% L_{coll} g/cm^2	Rad. length Fraction
Be	30.0	35.3	1.85	0.0556	0.00085
Al	25.5	8.9	2.70	0.069	0.0029
Ni	10.2	1.76	7.87	0.080	0.0058
Sn	13.2	1.21	7.31	0.096	0.011
Pb	4.8	0.56	11.35	0.111	0.018
U	6.2	0.32	18.95	0.117	0.019

TABLE 3

Target reaction cross sections and probabilities assuming an ^{16}O beam

Material	N target density (Nuclei/cm^2) $\times 10^{20}$ 0.1% L_{coll}	σ_T (10^{-26} cm^2)	N . σ_T (10^{-3})
Be	36.7	96	3.5
Al	15.3	138	2.1
Ni	8.57	182	1.6
Sn	4.8	251	1.2
Pb	3.2	323	1.0
U	2.9	345	1.0

TABLE 4

Targets thicknesses and interaction probabilities assuming a 13 GeVA ^{16}O beam and ≦ 10% for a secondary interaction

Target	Target thickness in collision lengths	Interaction probability
Be	4.0×10^{-3}	14.0×10^{-3}
Al	2.5×10^{-3}	5.3×10^{-3}
Ni	2.0×10^{-3}	3.0×10^{-3}
Sn	1.7×10^{-3}	2.0×10^{-3}
Pb	1.7×10^{-3}	1.7×10^{-3}
U	1.7×10^{-3}	1.7×10^{-3}

TABLE 5

Mean charged particle multiplicities and central rapidity density for pp and AA collisions

P_{beam} GeV/c	7.0	13.0	40.0	70.0	100.0	200.0
$\sqrt{s}$ GeV	3.9	5.1	8.8	11.5	13.8	19.4
η_o	2.9	3.6	5.0	5.9	6.4	7.6
ρ_o	0.65	0.78	1.05	1.18	1.27	1.44
$\bar{n}(16)$	46.0	58.0	80.0	94.0	102.0	122.0
$\bar{p}(16)$	10.4	12.5	16.8	18.9	20.3	23.0
$\bar{n}(40)$	116.0	144.0	200.0	236.0	256.0	304.0
p(40)	26.0	31.2	42.0	47.2	50.8	57.6

TABLE 6

Table of decay fractions

|S|	0	1				2		3
B($\bar{B}$)	(qqq)	(qqs)				(qss)		(sss)
	pn	Λ^o	Σ^+	Σ^o	Σ^-	Ξ^o	Ξ^-	Ω^-
cτ(cm)		7.9	2.4	0.0	4.4	8.7	4.9	2.5
Decay fractions		$p^+\pi^-$	$p^+\pi^o$	$\Lambda^o\gamma$	$n^o\pi^-$	$\Lambda^o\pi^o$	$\Lambda^o\pi^-$	$\Lambda^o K^-$
		0.64	0.52	1.0	1.0	1.0	1.0	0.69
		$n^o\pi^o$	$n^o\pi^+$					$\Xi^o\pi^-$
		.36	.48					0.23
								$\Xi^-\pi^-$
								0.08

TABLE 7

Decay survival efficiency

Table 7(a)

p_{beam} = 13 GeV/c, y^* = 0 $\frac{p_{||}}{M} \simeq 2.53$

y_{beam} = 3.323 y_{lab} = 1.66

Distance (cm)	20	30	50	100	150
Λ	0.37	0.22	0.081	0.0067	5.45×10^{-3}
Σ^+		7.2×10^{-3}	2.7×10^{-3}	7.0×10^{-8}	1.9×10^{-11}
Σ^-		0.069	0.012	1.4×10^{-4}	1.6×10^{-6}
Ξ^-		0.09	0.018	3.2×10^{-4}	5.9×10^{-6}
Ω^-		0.0087	3.7×10^{-4}	1.4×10^{-7}	5.0×10^{-11}

Table 7(b)

p_{beam} = 40, y^* = 0 $\frac{p_{||}}{M} \simeq 4.56$

y_{beam} = 4.45 y_{lab} = 2.22

Distance (cm)	20	30	50	100	150
Λ	0.56	0.43	0.25	0.062	1.5×10^{-2}
Σ^+	0.16	0.064	1.0×10^{-2}	1.1×10^{-4}	1.2×10^{-8}
Σ^-	0.37	0.23	0.085	7.2×10^{-3}	6.0×10^{-4}
Ξ^-	0.41	0.26	0.11	1.2×10^{-2}	1.2×10^{-3}
Ω^-	0.17	0.072	0.012	1.6×10^{-4}	1.9×10^{-6}

TABLE 7 (Cont'd)

Table 7(c)

$p_{beam} = 70$, $y^* = 0$ $\frac{p_{||}}{M} = 6.07$

$y_{beam} = 5.0$ $y_{lab} = 2.50$

Distance (cm)	20	30	50	100	150
Λ	0.66	0.53	0.35	0.12	0.044
Σ^+	0.25	0.128	0.032	1.0×10^{-3}	3.4×10^{-5}
Σ^-	0.48	0.33	0.157	0.024	3.8×10^{-3}
Ξ^-	0.51	0.37	0.187	0.035	6.6×10^{-3}
Ω^-	0.27	0.14	0.037	1.4×10^{-3}	5.1×10^{-5}

Table 7(d)

$p_{beam} = 200$ GeV/c, $y^* = 0$ $\frac{p_{||}}{M} = 10.3$

$y_{beam} = 6.05$ $y_{lab} = 3.02$

Distance (cm)	20	30	50	100	150	200
Λ	0.78	0.69	0.54	0.29	0.16	0.085
Σ^+	0.44	0.30	0.13	0.017	2.3×10^{-3}	3.0×10^{-4}
Σ^-	0.65	0.52	0.34	0.11	0.038	0.013
Ξ^-	0.67	0.55	0.37	0.14	0.052	0.019
Ω^-	0.46	0.31	0.14	0.02	3.0×10^{-3}	4.0×10^{-4}

TABLE 8

The topological efficiency of the detector to detect decays; A_D secondary Λ decays are considered for the Ξ and Ω decays

Table 8(a) Λ, $\bar{\Lambda}$ decays, $y^* = 0$

Beam GeV/c	P_p(50 cm) - P_p(150)	DF	A_D
13	0.081	0.64	0.052
40	0.235	0.64	0.150
70	0.306	0.64	0.196
200	0.38	0.64	0.24

Table 8(b) Σ^+ decays, $y^* = 0$

Beam GeV/c	P_p(50 cm) - P_p(150)	DF	A_D
13	2.7×10^{-4}	0.48	1.3×10^{-4}
40	1.0×10^{-2}	0.64	0.48×10^{-2}
70	0.031	0.48	0.015
200	0.13	0.48	0.062

Table 8(c) Σ^- decays, $y^* = 0$

Beam GeV/c	P_p(50 cm) - P_p(150)	DF	A_D
13	0.012	1.0	0.012
40	0.085	1.0	0.085
70	0.153	1.0	0.153
200	0.30	1.0	0.302

TABLE 8 (Cont'd)

Table 8(d) Ξ decays, $y^* = 0$

Beam GeV/c	P_p(50 cm) - P_p(150)	P_s	DF_p	DF_s	A_D
13	0.018	0.22	1.0	0.64	0.0106
40	0.10	0.75	1.0	0.64	0.048
70	0.152	0.65	1.0	0.64	0.063
200	0.23	0.46	1.0	0.64	0.302

Table 8(e) Ω decays, $y^* = 0$

Beam GeV/c	P_p(30 cm) - P_p(50)	P_s(50-150)	DF_p	DF_s	A_D
13	0.005	0.37	0.69	0.64	8.2×10^{-4}
40	0.60	0.56	0.69	0.64	0.015
70	0.103	0.66	0.69	0.64	0.03
200	0.23	0.78	0.69	0.64	0.058

Table 8(f) K^0_S decays, $y^* = 0$

Beam GeV/c	P_p(30 cm) - P_p(50)	P_p(50-100)	DF_p	A_D
13	0.012	6.2×10^{-4}	0.68	0.008
40	0.068	0.017	0.68	0.012
70	0.11	0.042	0.68	0.029
200	0.18	0.13	0.68	0.090

TABLE 9

Particle production multiplicities, $\langle B \rangle_{pp}$, for pp collisions [9]

p_{beam} (GeV/c)	13	40	75	200
$\sqrt{s}$ GeV	5.1	8.8	12.0	19.4
p	1.60	1.4	1.4	1.36
$\bar{p}$	1.5×10^{-3}	6.0×10^{-3}	15.0×10^{-3}	60×10^{-3}
Λ	3.6×10^{-2}	8.0×10^{-2}	12.0×10^{-2}	12×10^{-2}
$\bar{\Lambda}$	2.0×10^{-5}	1.7×10^{-3}	6.0×10^{-3}	26×10^{-3}
Σ^+	16.0×10^{-3}	40.0×10^{-3}	60.0×10^{-3}	60×10^{-3}
Σ^-	5.0×10^{-3}	15.0×10^{-3}	20.0×10^{-3}	30×10^{-3}
Ξ^- / Ξ^+	2.0×10^{-6}	1.7×10^{-4}	6.0×10^{-4}	4×10^{-3}
Ω^- / Ω^+		2.5×10^{-5}	9.0×10^{-5}	6×10^{-4}

TABLE 10

Detected particles per pulse per pp collision R, where

$$R = 10^{6} \cdot A \cdot \langle B \rangle_{pp} \cdot T$$

P_{beam}	A	T(X 10^{-3}) <B>pp (X 10^{-3})	Be 14.0	Al 5.3	Ni 3.0	Sn 2.0	Pb 1.7	U 1.7	Multi-plier
$\bar{p}$ 13	0.25	1.5	5.3	2.0	1.1	0.75	0.64	0.64	
40	0.25	6.0	21.1	8.0	4.4	3.0	2.6	2.6	
70	0.25	15.0	53.0	20.0	11.0	7.5	6.4	6.4	
200	0.25	60.0	121.0	80.0	44.0	30.0	26.0	26.0	
Λ 13	0.0125	36.0	6.3	2.4	1.4	0.90	0.76	0.76	
40	0.020	80.0	22.4	8.5	4.8	3.2	2.7	2.7	
70	0.017	120.0	28.0	10.6	6.0	4.0	3.4	3.4	
200	0.006	120.0	10.0	3.8	2.2	1.4	1.2	1.2	
$\bar{\Lambda}$ 13	0.0125	0.02	35.0	13.3	7.5	5.0	4.3	4.3	$\times 10^{-4}$
40	0.020	1.7	0.48	0.18	0.10	0.068	0.058	0.058	
70	0.017	6.0	1.44	0.54	0.3	0.20	0.17	0.17	
200	0.006	26.0	2.2	0.83	0.47	0.31	0.27	0.27	
Σ^{+} 13	9.0×10^{-6}	16.0	20.0	7.6	4.3	2.8	2.4	2.4	$\times 10^{-4}$
40	10^{-4}	40.0	56.0	21.0	12.0	8.0	6.8	6.8	$\times 10^{-3}$
70	3.0×10^{-4}	60.0	25.0	9.5	5.4	3.6	3.1	3.1	$\times 10^{-2}$
200	12.0×10^{-4}	60.0	1.0	0.38	0.22	0.14	0.12	0.12	
Σ^{-} 13	3.0×10^{-3}	5.0	0.21	0.08	0.045	0.03	0.026	0.026	
40	21.0×10^{-3}	15.0	4.4	1.7	0.95	0.63	0.54	0.54	
70	38.0×10^{-3}	20.0	10.6	4.0	2.3	1.5	1.3	1.3	
200	76.0×10^{-3}	30.0	32.0	12.0	6.8	4.6	3.9	3.9	
Ξ^{-} 13	2.7×10^{-3}	0.002	7.61	2.9	1.6	1.1	0.92	0.92	$\times 10^{-5}$
40	12.0×10^{-3}	0.17	28.0	10.6	6.0	4.0	3.4	3.4	$\times 10^{-3}$
70	16.0×10^{-3}	0.60	140.0	53.0	30.0	20.0	17.0	17.0	$\times 10^{-3}$
200	17.0×10^{-3}	4.0	0.95	0.36	0.20	0.13	0.12	0.12	
Ω^{-} 13	2.0×10^{-4}	-							
40	37.0×10^{-4}	0.025	130.0	49.0	28.0	19.0	16.0	16.0	$\times 10^{-5}$
70	75.0×10^{-4}	0.090	9.5	3.6	2.0	1.3	1.2	1.2	$\times 10^{-3}$
200	145.0×10^{-4}	0.60	122.0	46.0	26.0	17.0	15.0	15.0	$\times 10^{-3}$
K^{o}_{s} 13	1.9×10^{-3}	37.0	1.0	0.4	0.2	0.14	0.12	0.12	
40	1.6×10^{-3}	80.0	1.8	0.7	0.4	0.26	0.22	0.22	
70	2.5×10^{-3}	110.0	3.9	1.5	0.8	0.55	0.47	0.47	
200	2.2×10^{-3}	190.0	5.9	2.2	1.3	0.84	0.71	0.71	

FIGURE CAPTIONS

Fig. 1 Layout of experiment for 13 GeVA ^{16}O ions.

Fig. 2 Efficiency of detector system to observe strange baryon decays A_D as a function of laboratory momenta.

Fig. 3 Monte-Carlo event simulation superimposing 4pp, 4nn, 4np, 4pn collisions at a beam momentum of 13 GeV/c/nucleon. We show here only the charged particles which appear somewhere in the μTPC. The e^+e^- pair is from the interaction of a γ at the boundary of the filter magnet. The event had a total of 137 tracks, charged plus neutrals. The view is in the plane containing the magnetic bends in both the filter magnet and the dipole magnet.

Fig. 4 Some event simulation as in fig. 3. View is in three dimensions.

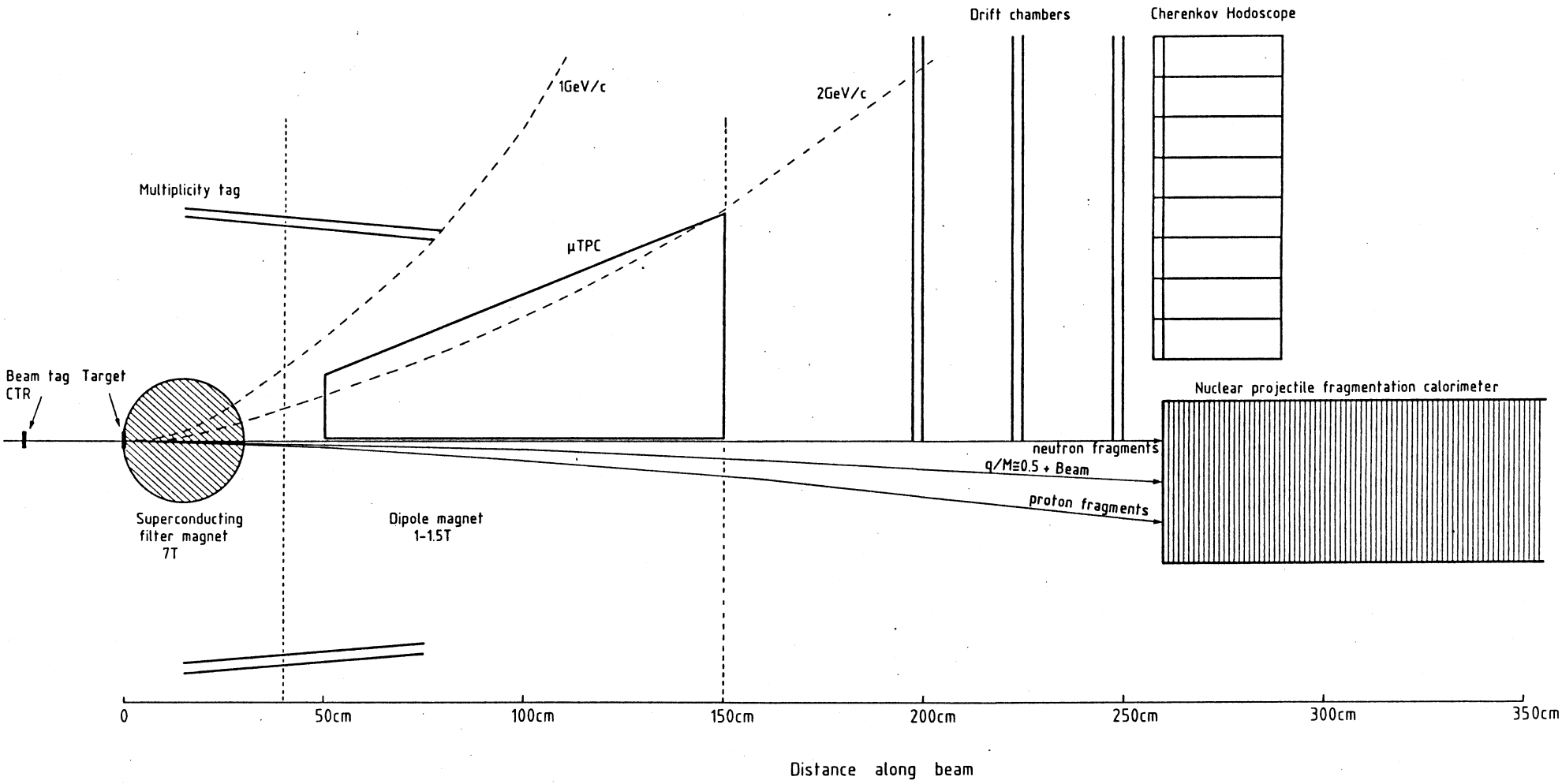
Drift chambers
Cherenkov Hodoscope
1GeV/c
2GeV/c
Multiplicity tag
μTPC
Beam tag
CTR
Target
Nuclear projectile fragmentation calorimeter
neutron fragments
q/M≅0.5 + Beam
proton fragments
Superconducting
filter magnet
7T
Dipole magnet
1-1.5T
0
50cm
100cm
150cm
200cm
250cm
300cm
350cm
Distance along beam

Fig. 1

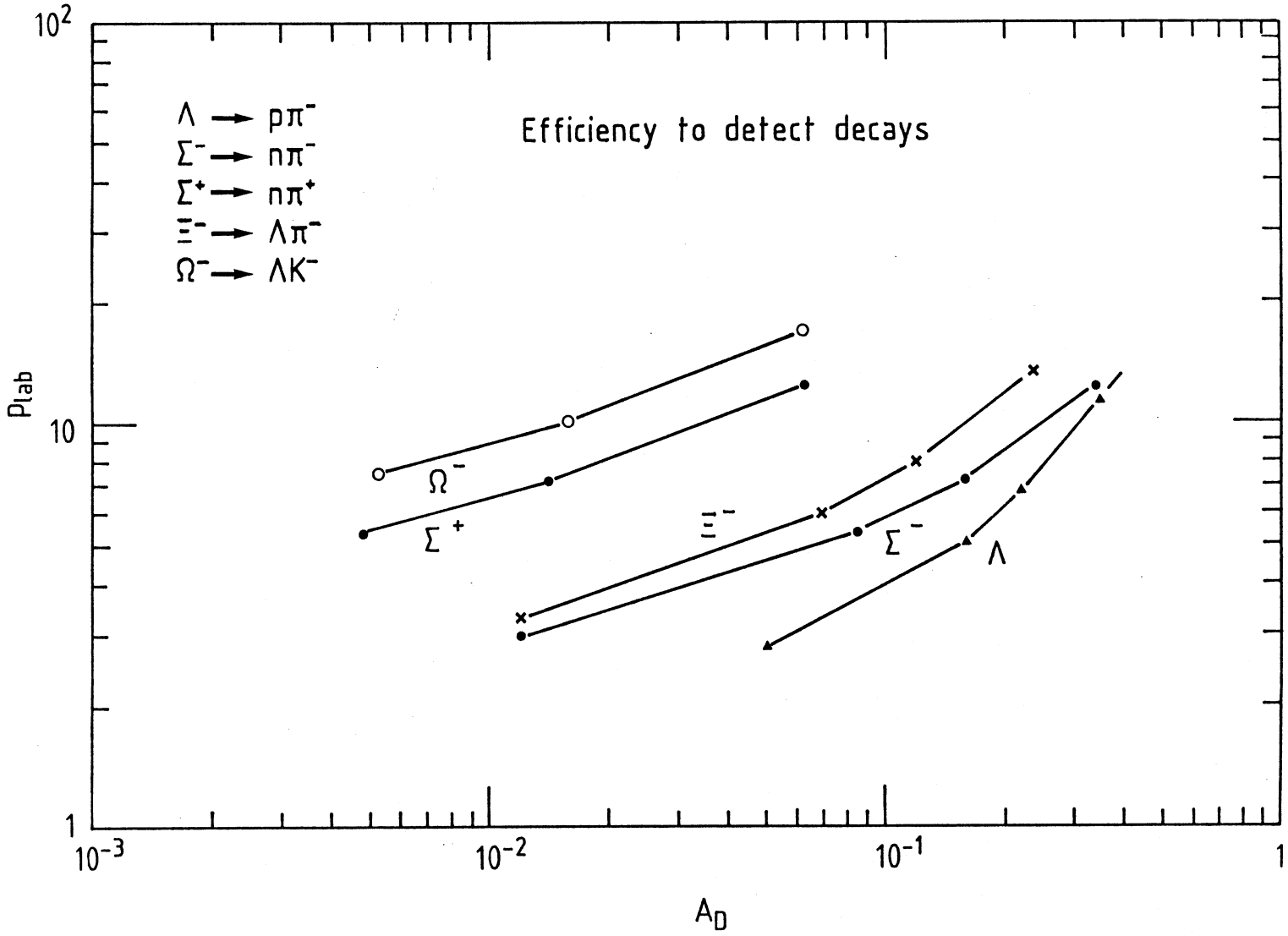
Efficiency to detect decays
Λ → pπ⁻
Σ⁻ → nπ⁻
Σ⁺ → nπ⁺
Ξ⁻ → Λπ⁻
Ω⁻ → ΛK⁻
Ω⁻
Σ⁺
Ξ⁻
Σ⁻
Λ
p_lab
A_D
10²
10
1
10⁻³
10⁻²
10⁻¹
1

Fig. 2

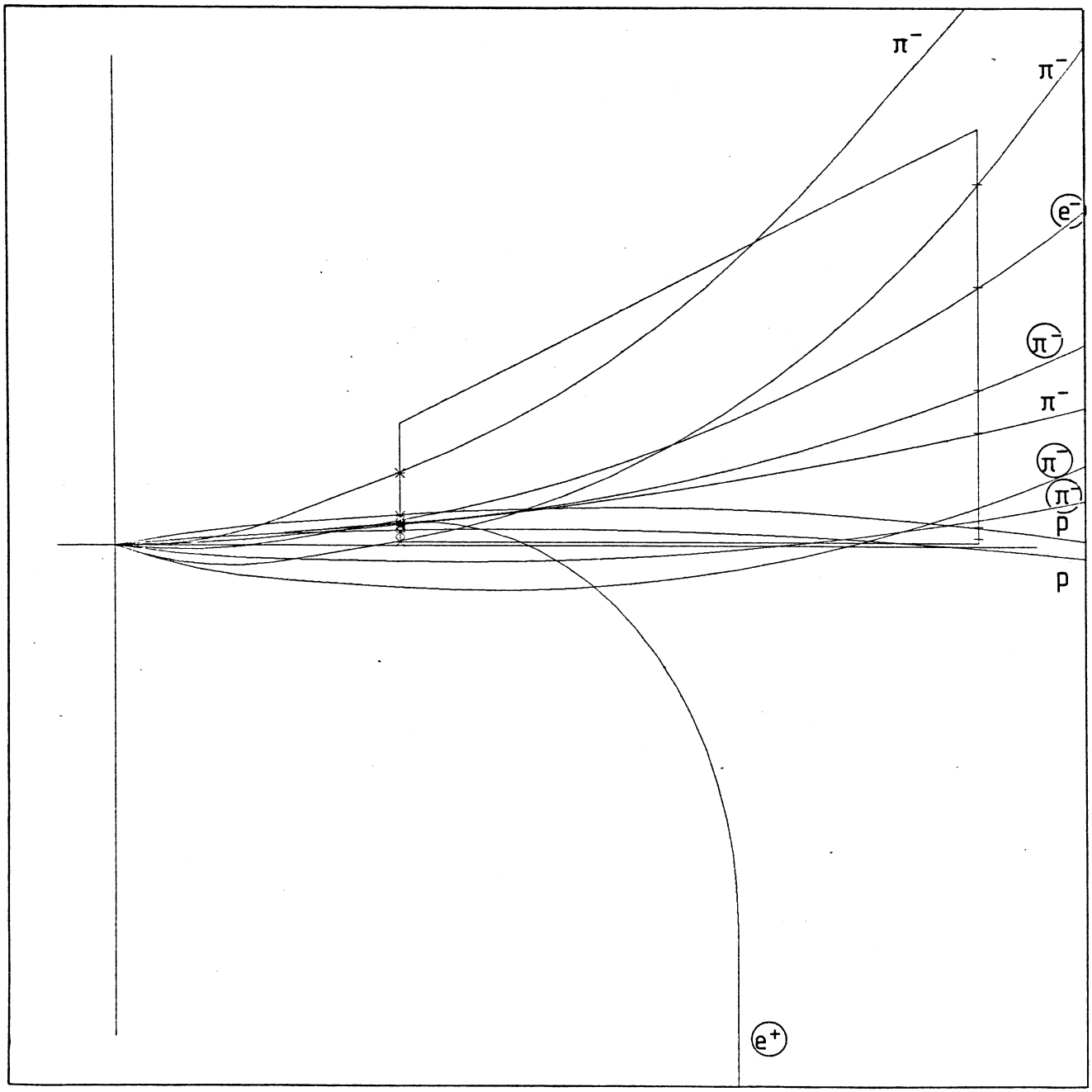

Fig. 4

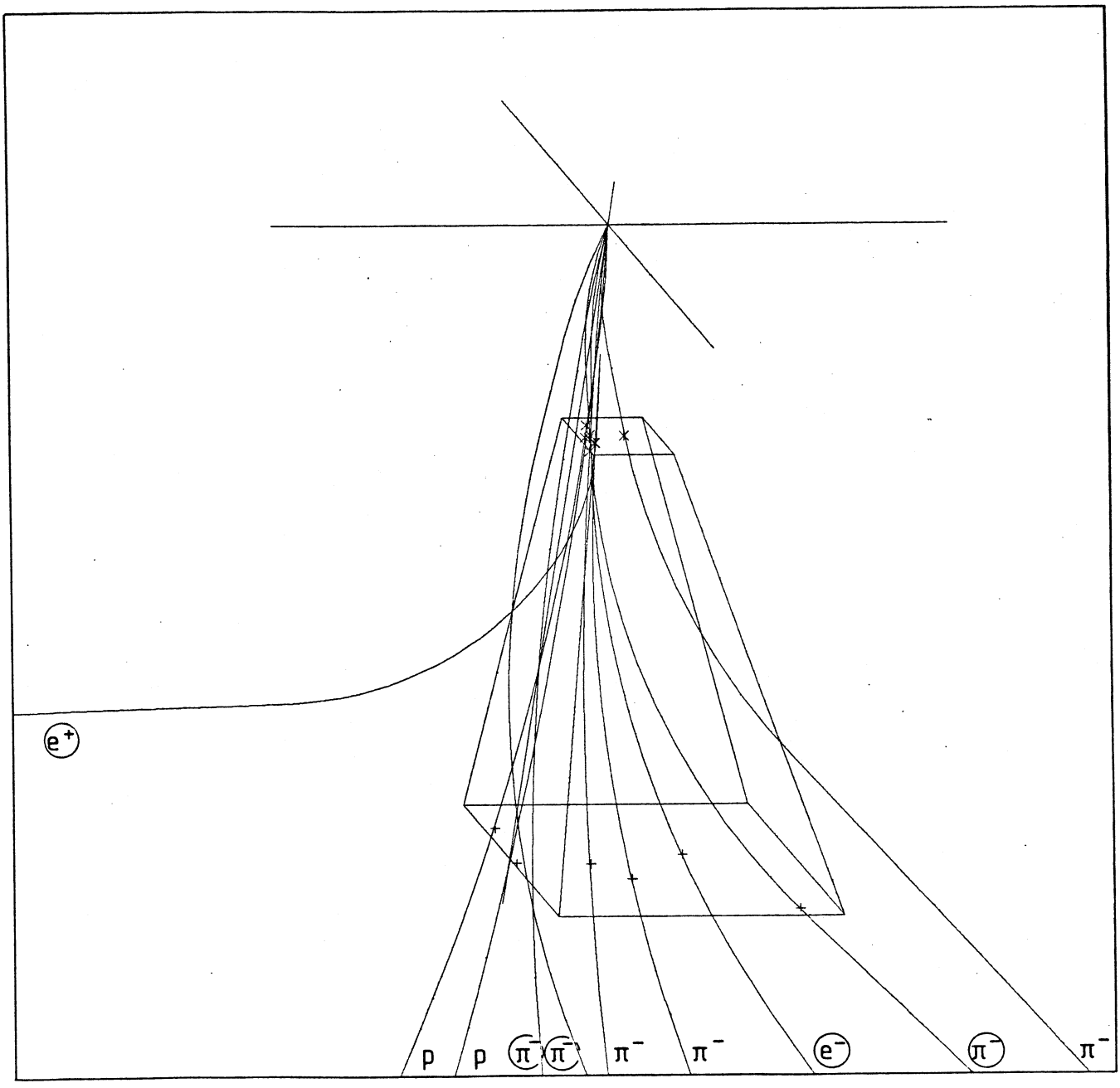

Fig. 3